POSITIVE PION-PROTON SCATTERING AT THE ENERGIES 176, 200, 240, 270, 307 AND 310 MEV

A. I. MUKHIN, E. B. OZEROV, B. M. PONTEKORVO, E. L. GRIGORIEV and N. A. MITIN

Institute of Nuclear Problems, USSR

(presented by A. I. Mukhin)

Introduction

At present there is a lack of precise data on angular distribution of π^+-mesons, elastically scattered by hydrogen. Most of the data published refer to energies less than 200 Mev[1–5]. This is due to difficulties connected with obtaining on cyclic accelerators sufficiently intensive and monoenergetic beams of high energy positive pions. Measurements made by the diffusion chamber method up to an energy of 400 Mev [6] do not have sufficient statistical accuracy.

In the Institute of Nuclear Problems of the USSR Academy of Sciences the possibility of obtaining intense beams of high energy positive pions arose only after the proton beam with an energy of about 660 Mev and with a density $\sim 10^9$ cm^{-2} sec^{-1}[7] was extracted from the synchrocyclotron chamber.

In this report an account is given of the results obtained by studying the scattering of π^+ mesons by hydrogen at pion energies 176, 200, 240, 270, 307 and 310 Mev. At 310 Mev measurements were made with photoplates, and at remaining energies with scintillation counters.

Meson beams

Positive meson beams were obtained by bombardment of a polyethylene target with a proton beam extracted

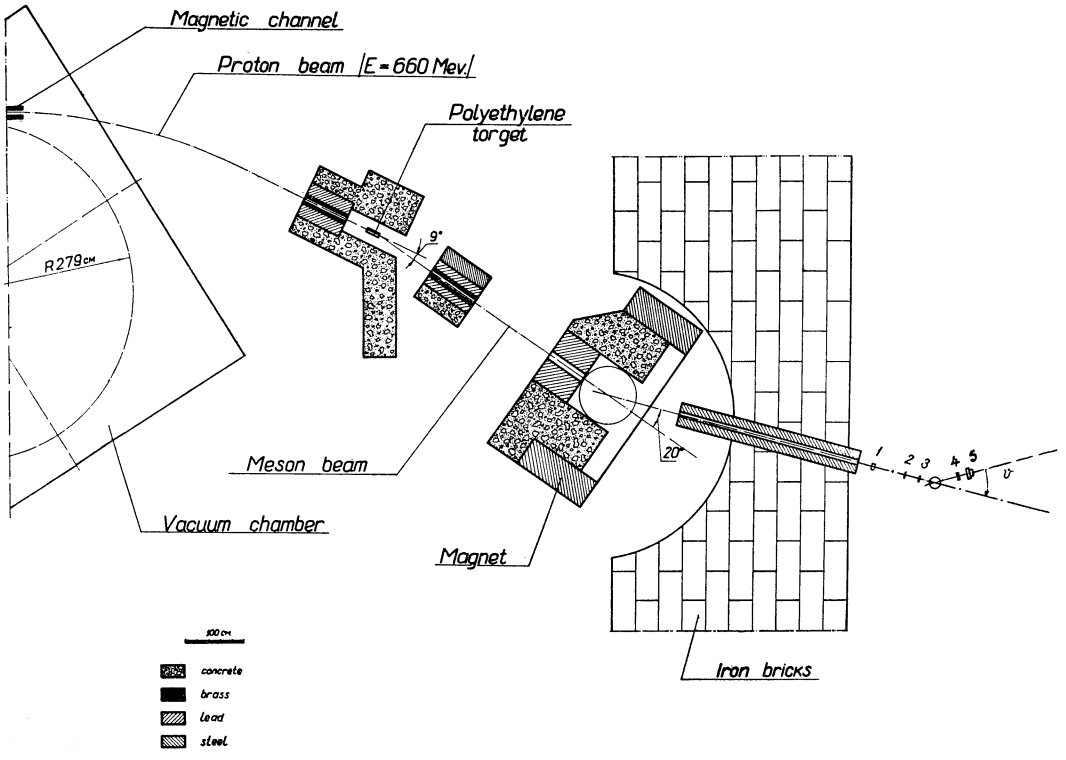

Fig. 1. Experimental arrangement.

from the synchrocyclotron. Mesons produced in the reaction $p+p\rightarrow\pi^+ +d$ at 9° to the direction of the proton beam were deflected with a magnet by 20° and having passed through a four-meter iron collimator with an inner diameter equal to 5 cm. were detected by the registering equipment situated behind the main shielding wall of the synchrocyclotron (fig. 1). In the experiments made with scintillation counters for each desired meson energy determined by the magnitude of the magnetic field of the deflecting magnet, the thickness of the polyethylene target was chosen experimentally so as to obtain the highest possible meson fluxes. The optimum thickness of the polyethylene target for energies 176, 200, 240, 270 and 307 Mev was respectively about 67 gm/cm², 53 gm/cm², 35 gm/cm², 19 gm/cm² and 4.6 gm/cm². The corresponding meson fluxes were roughly equal to 20 cm^{-2} sec^{-1}, 40 cm^{-2} sec^{-1}, 60 cm^{-2} sec^{-1}, 60 cm^{-2} sec^{-1} and 40 cm^{-2} sec^{-1}.

It is noteworthy that in spite of the considerable thicknesses of the polyethylene target used there is a comparatively narrow peak (fig. 2) from the reaction $p+p\rightarrow\pi^+ +d$ in the curve giving the intensity Φ of the meson beam as a function of the deflecting magnet current I_M. This may be explained by the fact that the mesons created in the "front" part of the target and slowed down in the target have roughly the same energy as the mesons produced by moderated proton beams on their way out of the "rear" part of the target. Accurate energy determination in each case was made by measuring the meson range in copper. A typical absorption curve for mesons with an energy of 307 Mev is shown in fig. 3. To the range measured by the absorption curve a correction, as in previous papers [8], was applied, which took into account the multiple Coulomb scattering of mesons in copper. For all energies this correction is about 2.5 per cent and does not practically vary with changes in the energy. The final energy values shown in Table I take into account the energy losses of mesons in the Dewar walls and in the hydrogen. They correspond to meson energies in the centre of the hydrogen target. The energy uncertainty is due mainly to the uncertainty in range determination, to the initial beam non-uniformity and also to the uncertainty of the range-energy curve. The μ meson contamination which is also shown in Table I was determined by using known data on nuclear interaction of pions in copper.

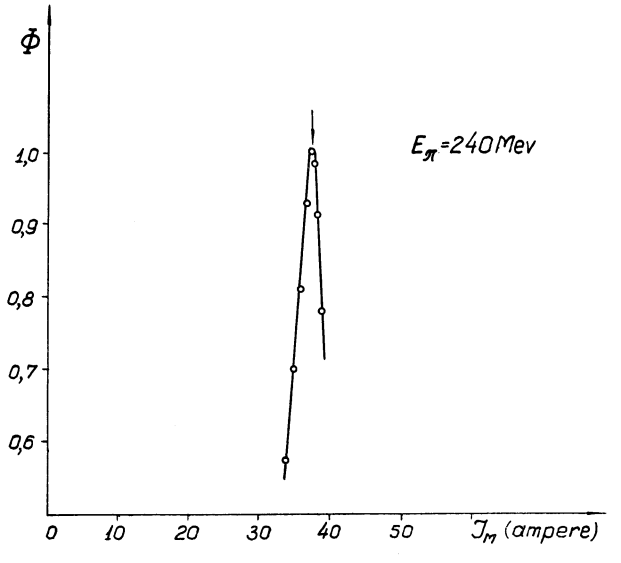

Fig. 2. Dependence of the meson flux Φ upon the deflecting magnet current J_M for a polyethylene target 35 gr/cm² thick.

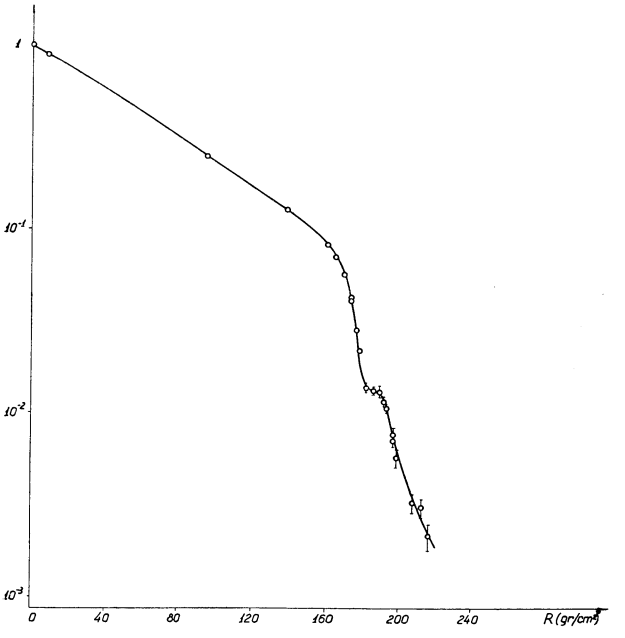

Fig. 3. A typical integral range curve (E_π = 307 Mev).

TABLE I

Corrected range of π^+ mesons in copper (gm/cm²)	Energy of π^+ mesons at the centre of the hydrogen scatterer (Mev)	Uncertainties in energy of mesons interacting with hydrogen	Contamination of μ^+ mesons (per cent)
90.4	176	±4	4.7±1.5
106.6	200	±5	4.0±1.0
134.1	240	±6	3.7±1.0
155.2	270	±6	3.4±1.0
180.4	307	±6	2.6±1.0

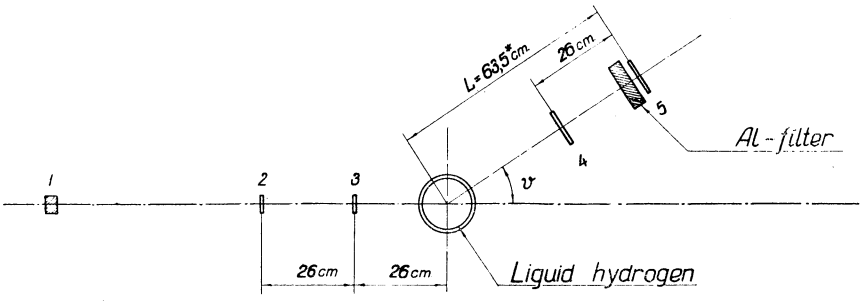

*for ϑ=20° L=73.5 cm.
1-Čerenkov detertor
2,3,4 5-Scintillation counters.

Fig. 4. Geometry used in angular distribution experiments.

Experimental arrangement

A. Angular distribution

The geometry used in measuring angular distributions is given in fig. 4. In the experiments a Čerenkov detector 1 and liquid scintillation counters 2 and 3 were used in coincidence to register the number of π^+ mesons falling on the hydrogen target (monitor). The Čerenkov detector was chosen because the meson beam contains a considerable number of slow protons. Scattered mesons were detected by liquid scintillation counters 4 and 5 in coincidence with counters 1 and 3. The block-diagram of the electronics system is shown in fig. 5. The resolving time of the triple and quadruple coincidence schemes was equal to 1.5×10^{-8} sec. The stability of the electronic apparatus operation was systematically controlled by measuring the ratio of the quadruple coincidence number (1, 3, 4, 5) to the triple coincidence number (1, 2, 3). For this purpose counters 4 and 5 were placed in a line with counters 1, 2 and 3.

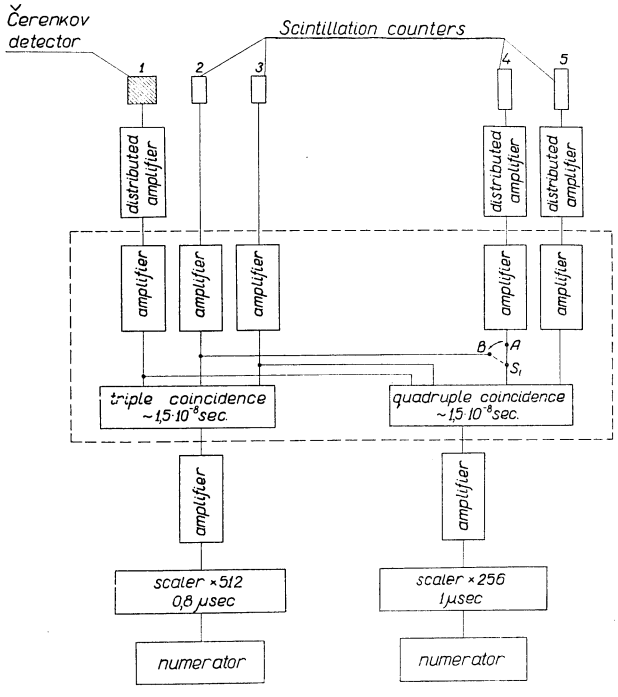

Fig. 5. A block diagram of the electronics system.

The Čerenkov detector was made of plexiglass and was connected to a photomultiplier by a plexiglass light-pipe. The scintillation counters 2 and 3 had the dimensions – 5 cm. × 5 cm. × 0.6 cm. and were made of a thin-wall plexiglass container filled with a solution of terphenyl in phenylcyclohexane. Counters 4 and 5 had a diameter and thickness of scintillating matter (a solution of terphenyl in phenylcyclohexane) of 10 cm. and 0.8 cm. respectively. The scintillators were likewise connected to a photomultiplyer by light-pipes.

A Dewar flask with an interior diameter of about 14 cm. and a thickness of walls equal to 1 gm/cm² was used as a hydrogen target. With a 3 litre capacity of the Dewar flask and a rate of hydrogen evaporation of about 0.25 litres per hour no liquid hydrogen was added during continuous 8 hours' work. During background experiments (without hydrogen) the Dewar was evacuated.

In determining the quantity of hydrogen it was assumed that the density of liquid hydrogen is equal to 0.0708 gm/cm³. Considering the rate of evaporation of hydrogen to be comparatively small, the influence of bubbles on the density was disregarded. The mean quantity of hydrogen on the path of the meson beam was 0.984 gm/cm² with an uncertainty of about one per cent.

In order to avoid detection of charged particles from stars occuring in the Dewar walls and also proton recoils from (π^+, p) scattering, aluminium filters were placed between the scintillators 4 and 5.

Angular distributions were obtained from the ratio $\frac{N_4}{N_3}$ after taking into account the efficiency of meson detection at various angles and a series of additional corrections which will be discussed in the following chapters.

B. Total cross sections

Total cross sections of π^+ mesons in hydrogen were measured by attenuation of the meson beam after passing through the hydrogen scatter (fig. 6). As in previous experiments [9] on total cross sections the distance from the centre of the hydrogen scatterer to the last scintillator was equal to 35 cm., which corresponds to an average registration angle for the last detector close to 8°.

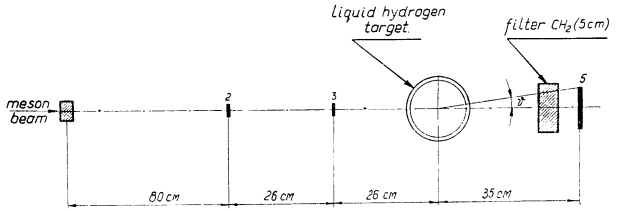

Fig. 6. Geometry for measuring total cross sections in trans mission experiments.

The mesons falling on the hydrogen target were detected by a system of three counters 1, 2 and 3 connected in coincidences. The beam transmitted through the scatterer was registered by quadruple coincidences (1, 2, 3, 5). The electronic block-scheme for these experiments is also shown in fig. 5.

The scintillators 2 and 3 used in these experiments had a diameter of 3 cm. and thickness of 0.4 cm. They were made of thinwalled plexiglass containers filled with a solution of terphenyl in phenylcyclohexane. Scintillator 5 as previously had a diameter of 10 cm.

The hydrogen target was the same as that used in measuring angular distributions.

Method of measuring angular distributions

I. *Scintillation counter experiments*

Differential cross sections in the laboratory system were determined by the formula

$$\left(\frac{d\sigma}{d\Omega}\right)_{lab} = \frac{N_4}{K \cdot N_3} \cdot \frac{1}{N_H \cdot \varepsilon \cdot \Omega}$$

where

N_4 is the number of mesons scattered by hydrogen at a given angle ϑ which are registered by quadruple coincidences;

N_3 is the number of triple coincidences;

K is a factor characterizing the beam;

N_H is the number of hydrogen atoms per cm^2;

ε is the efficiency of registration of mesons at the angle ϑ;

Ω is the effective solid angle.

A description of experiments designed in order to find the parameters appearing in the formula is given below. The numerical values of these parameters will be given in the tables which summarize the experimental results.

A. Determination of π^+ meson flux

In view of the fact that in the scattering experiments a thick hydrogen target was used, it was necessary to take into account the absorption of mesons not only in scintillator 3 and in the front walls of the Dewar but also in the hydrogen scatterer. In determining the number of mesons falling on the hydrogen target, counting losses, which are especially important at energies 240 and 270 Mev, were taken into account.

Finally it was necessary to consider the mu-contamination of the beams.

Taking into account the above mentioned facts the mean number of π^+ mesons N_π that could take part in the scattering was determined as follows:

$$N_\pi = kN_3 = N_3 \cdot \eta \cdot \alpha_\pi \left\{ 1 - \frac{1}{2} e^{-\sigma_t N_H} - \beta \right\}$$

Here η is a coefficient taking into account counting losses in the registration of triple coincidences;

α_π is the fraction of π mesons in the beam;

σ_t is the total cross section of π^+ mesons in hydrogen;

β is the fraction of the beam absorbed in scintillator 3 and in the front walls of the Dewar.

B. Efficiency of meson registration

The efficiency of registration of mesons scattered under different angles and detected by quadruple coincidences (1, 3, 4, 5) is determined by two factors:

1. The registration probability of mesons which passed through the sensitive volume of the scintillation counters 4 and 5, and
2. the absorption probability in the scintillator 4 and in the aluminium filter of mesons scattered at a given angle.

Both the absorption of scattered mesons and their registration probability were determined in special experiments. The first factor was determined by experiments performed in the geometry shown in fig. 7. It was found

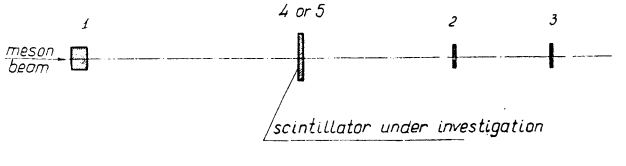

Fig. 7. Experimental arrangement for investigating pion detection probabilities in scintillators 4 and 5.

that the probabilities of registering mesons by scintillators 4 and 5

$$\varepsilon_4 = \frac{N_4\,(1,2,3,4)}{N_3\,(1,2,3)} \text{ and } \varepsilon_5 = \frac{N_4\,(1,2,3,5)}{N_3\,(1,2,3)}$$

are equal to unity with an accuracy of a few tenths of one per cent.

The four counter coincidence system 1, 3, 4 and 5 had a very good plateau (the counting rate varied only by 1 per cent when the voltage changed by 200-300 volts).

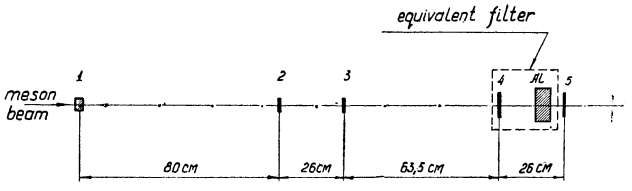

Fig. 8. Geometry used in determining meson attenuations in filters.

In order to measure the absorption of scattered mesons in the "equivalent filters" consisting of scintillator 4 and aluminium filter, counters 1, 2, 3 and 5 were arranged in one line. The attenuation of meson beams in these equivalent filters was determined for a number of energies. The electronic scheme variant (fig. 5) designated for measuring total cross sections was used. The geometry of the experiment is shown in fig 8. In this experiment the meson beam energy was defined by the current in the deflecting magnet. Control measurements performed when measuring ranges in copper showed that discrepancies between energy values determined by the two methods did not exeed $\pm$ 2 Mev.

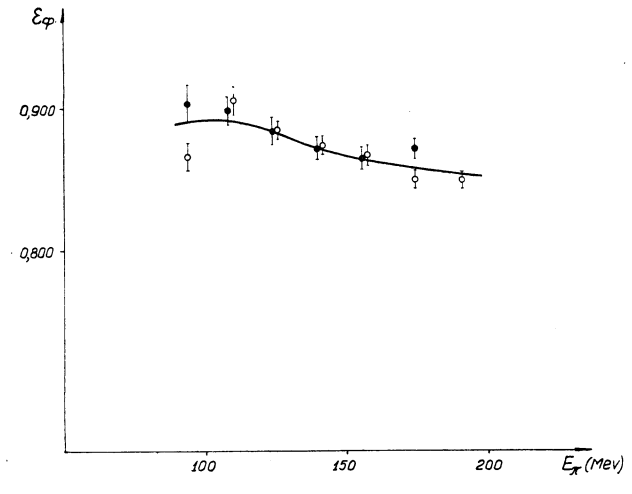

Fig. 9. Meson detection efficiency as a function of pion energy energy (Al filter 3 cm. thick).

From the measurements of $\varepsilon_\varphi = \frac{N_4\ (\text{filter})}{N_4\ (\text{without filter})}$ as a function of energy for Al filters of different thicknesses it is evident that in the region of energies close to 200 Mev ε_φ (E) has a minimum due to the character of the energy dependence of total pion cross sections for complex nuclei [10].

From absorption curves in Al at different energies it was possible to measure directly the detection efficiency of scattered mesons, since the probability of meson registration in scintillators 4 and 5 is equal to one.

A slight correction to the detecting efficiency was applied to take into account the absorption of scattered mesons in the wall of the hydrogen target.

Thus the registration efficiency of scattered mesons, given in Tables II-VI, was determined as

$$\varepsilon = \varepsilon_\varphi\ (1 - x),$$

where x is the fraction of scattered mesons absorbed by the Dewar walls.

C. Determination of the effective solid angle

The most important geometrical correction was introduced due to the fact that the dimensions of scintillator 4 were less than the diameter of the hydrogen target. Consequently there is an angle-dependent part of the hydrogen scatterer which is located in a half-shade in relation to the telescope of counters 4-5; fig. 10 gives the dependence on angle ϑ of the ratio $\frac{\Omega_{av}}{\Omega_c}$ (Ω_c is the solid angle through which scintillator 5 is seen from the centre of the hydrogen target and Ω_{av} is the solid angle defined by the telescope of scintillation counters 4-5, averaged over the volume of the scatterer).

In order to obtain the effective solid angle for the registration of scattered mesons it is necessary to apply to Ω_{av} an additional correction taking into account scat-

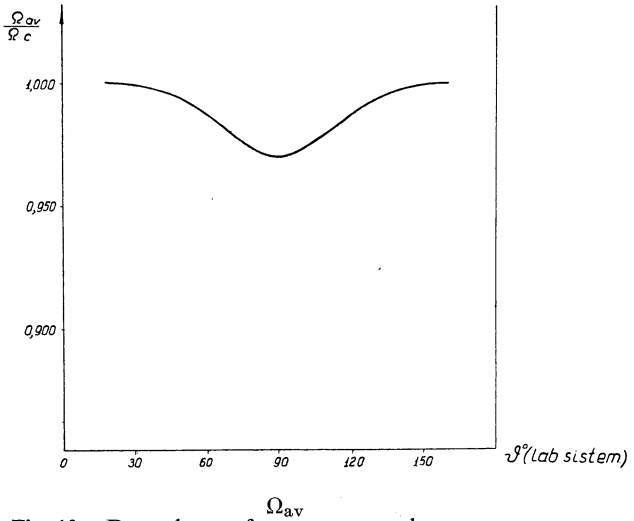

Fig. 10. Dependence of $\frac{\Omega_{av}}{\Omega_c}$ upon angle.

tered meson detection in the light-pipe of scintillation counter 5.

The comparatively high sensibility of plexiglass light pipes to high energy particles is due both to Čerenkov radiation and to "weak" scintillations in the plexiglass.

The increase of the average solid angle $\frac{\Omega - \Omega_{av}}{\Omega_{av}}$ was determined for mesons of known energies scattered under two angles. The dependence of the light-pipe sensitivity on energy was determined in the direct meson beam for different values of the deflecting magnet current. This made it possible to obtain the effective value of the solid angle Ω necessary for the determination of the differential cross-sections given in this report. The dependence of the average increase in the solid angle on meson energy is shown in fig. 11. While determining the effective solid angle another correction was applied taking into account the fact that the telescope of scintillation counters 4-5 has a limited angular resolution.

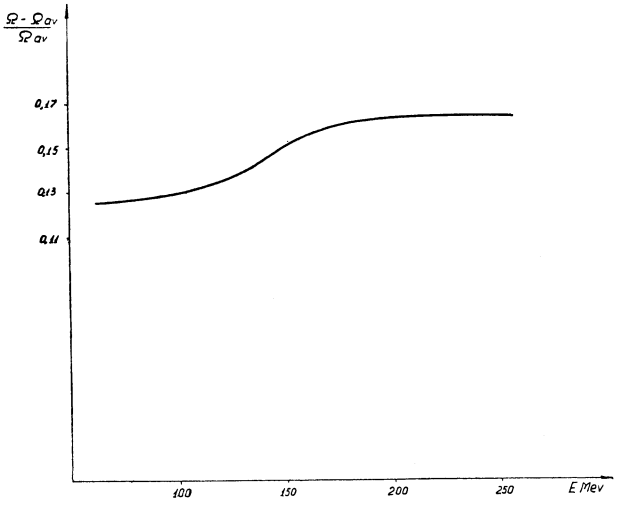

Fig. 11. Energy dependence of $\frac{\Omega - \Omega_{av}}{\Omega_{av}}$

Multiple nuclear meson scattering in hydrogen was not taken into account. Likewise no account was taken, because of their insignificance, of corrections connected with chance coincidences and with π-μ decay of scattered mesons.

II. *Photoplates*

Electron-sensitive photoplates with an emulsion layer 400 micron thick were exposed to the π^+ meson beam at the outlet of a four-meter collimator. In order to shield the plates from protons in front of the plates a copper filter 2 cm. thick was placed. After their transmission through the filter the meson energy was 310 ± 10 Mev.

Scattering events were looked for by area scanning with immersion lenses and a magnification of 450 ×. In order to obtain good registration efficiency of scattering events scanning of the entire area was repeated. In order to determine the scanning efficiency which is somewhat different for various scattering angles, a part of the photo-plate area was carefully scanned with a magnification of 630 ×. Corrections introduced on the basis of results obtained after such a scanning refer to angles greater than 110° in the centre of mass system and did not exceed 4-5 per cent. Moreover, in order to check the scanning efficiency the number of stars created by π^+ mesons in the photoemulsion was counted. If the cross-section of π^+ meson interaction with nuclei is close to the geometrical cross-section, then for every 13-14 stars one elastic scattering of π^+ meson on hydrogen must be observed. Results obtained by such a method of checking indicate that the scanning efficiency was very high indeed.

Elastic scattering processes were identified by the following criteria arising from the laws of energy and momentum conservation.

1. The angular correlation between the scattered meson and the proton recoil. All cases in which the angular correlation differed from the computed one by more than 1° were disregarded.

2. Coplanarity. Conditions of coplanarity are fulfilled when

$$\sin \Phi = \frac{\cos \delta_0 \cdot \cos \delta_1 \cdot \cos \delta_2}{\sin \vartheta'} \times$$

$$\times \left[\operatorname{tg} \delta_1 \cdot \sin \vartheta'_2 - \operatorname{tg} \delta_2 \cdot \sin \vartheta'_1 + \operatorname{tg} \delta_0 \cdot \sin (\vartheta'_1 - \vartheta'_2) \right],$$

where δ_0, δ_1 and δ_2 are the angles of inclination to the emulsion plane of the primary, scattered meson and proton recoil track, respectively: ϑ'_1, ϑ'_2 are the meson scattering angle and the angle of the proton recoil, respectively, in the emulsion plane; ϑ' is the angle in the emulsion plane between the scattered meson and the recoil proton;

Φ is the angle of inclination of the primary meson track to the plane of the scattered meson and recoiling proton tracks.

Events in which $\Phi > 1°$ were neglected, since they did not satisfy coplanarity conditions. For small angle scattering when the recoiling proton possesses a low energy and stops in the emulsion it was required that its energy should be equal to the computed one.

Scattering events produced by mesons whose tracks deviated from the initial direction of the meson beam by angles greater than 3° (the mean angle of multiple scattering in the copper filter) were neglected.

The angular distribution obtained (interval of summation equal to 20°) was normalised so that

$$\int \frac{d\sigma}{d\Omega} d\Omega = \sigma_t (\pi^+, p)$$

where σ_t (π^+, p) is the total cross-section of π^+ mesons in hydrogen. It was assumed that the total cross-section at 310 Mev is equal to 70×10^{-27} cm^2 [11].

Method used in measuring total cross-sections

Total pion-proton cross-sections, measured by the method of attenuation of the beam passing through the scatterer, were determined by the formula :

$$\sigma_t(\pi^+, p) = \frac{1}{N_H} \ln \left\{ \frac{N_4^{(noH)} \cdot \eta^{(noH)} - N_4^{(0)} \cdot \eta^{(0)} \cdot \alpha_\mu}{N_4^{(H)} \cdot \eta^{(H)} - N_4^{(0)} \cdot \eta^{(0)} \cdot \alpha_\mu} \right\} + \int_0^{\vartheta = 8^0} \left\{ \left(\frac{d\sigma_\pi}{d\Omega} \right)_{lab} + \left(\frac{d\sigma_p}{d\Omega} \right)_{lab} \right\} d\Omega$$

The following notations were used :

$N_4^{(0)}$, $N_4^{(noH)}$ and $N_4^{(H)}$ – number of quadruple coincidences normalized to unity of monitor, respectively, without Dewar $[N_4^{(0)}]$; with evacuated Dewar $[N_4^{(noH)}]$ and with the Dewar filled with liquid hydrogen $[N_4^{(H)}]$

$\eta^{(0)}$, $\eta^{(noH)}$ and $\eta^{(H)}$ — factors taking into account the counting losses in the registering system :

α_μ — fraction of μ mesons in the beam;

$\left(\frac{d\sigma_\pi}{d\Omega} \right)_{lab}$ — angular distribution of π mesons in the laboratory system of coordinates;

$\left(\frac{d\sigma_p}{d\Omega} \right)_{lab}$ — angular distribution of recoiling protons in the laboratory system of coordinates.

Accidental coincidences determined in separate experiments were negligibly small (of the order of 0.1 per cent).

Experimental results

A. Differential cross-sections

The experimental results are tabulated below. In Tables II-VI are shown the results of measurements made with scintillation counters. In addition to the final values of differential cross sections in the laboratory system $\left(\frac{d\sigma}{d\Omega} \right)_{lab}$ and in the center of mass system $\frac{d\sigma}{d\Omega}$, numerical values of the already defined parameters K, Ω and ε are given in the tables. An idea of the background under different angles (without hydrogen) may be obtained from the fourth column, where the ratio $\frac{N_4 \text{ (Dewar)}}{N_4 \text{ (Dewar + H)}}$ of the normalized number of quadruple coincidences without and with hydrogen in the Dewar is given. The fifth column gives the counting rate (N_4 (Dewar + H) — N_4 (Dewar)) of quadruple coincidences due to hydrogen only and normalized to 10^6 counts of triple coincidences N_3.

Errors in the final cross section are standard deviations. They include uncertainties in the determination of corrections and ultimately have only a statistical nature.

TABLE II $E_\pi = 176 \pm 4$ Mev

Angular distribution of π^+ mesons scattered by hydrogen

Angle ϑ in the laboratory system (degree)	Distance from the centre of the target to last scintillator (cm.)	Thickness of aluminium filter (cm.)	Approximate magnitude of background $\frac{N_4 \text{ (Dewar)}}{N_4 \text{ (Dewar+H)}}$	"Net" hydrogen effect (per 10^6 countings of monitor)	K factor characterising the beam	Ω effective solid angle in the laboratory system. (sterad.)	ε detection efficiency for scattered mesons	$\left(\frac{d\sigma}{d\Omega} \right)_{lab}$ lab. differential cross-sections in the laboratory system (10^{-27} cm^2 sterad^{-1})	Angle θ in the centre of mass system. (degree)	$\frac{d\sigma}{d\Omega}$ differential cross-sections in the centre of mass system (10^{-27}cm^2 sterad^{-1})
30	63.5	3.8	0.4	308±30	0.915	2.20×10^{-2}	0.835	31.1±3.1	38.5	20.0±2.0
45	63.5	3.0	0.2	221±20	0.915	2.16×10^{-2}	0.858	22.1±2.1	56.8	15.7±1.5
60	63.5	3.0	0.14	129±14	0.915	2.17×10^{-2}	0.867	12.7±1.4	74.2	10.2±1.1
75	63.5	3.0	0.17	96±11	0.915	2.13×10^{-2}	0.879	9.6±1.1	90.4	8.8±1.0
90	63.5	0.8	0.17	105±13	0.915	2.10×10^{-2}	0.912	10.2±1.3	105.6	10.8±1.4
105	63.5	0.8	0.13	128±14	0.915	2.10×10^{-2}	0.904	12.5±1.4	119.5	15.3±1.7
120	63.5	0.8	0.16	142±15	0.915	2.11×10^{-2}	0.900	13.9±1.5	132.9	19.3±2.1
135	63.5	0.8	0.22	146±15	0.915	2.13×10^{-2}	0.898	14.2±1.5	145.3	21.8±2.3
149	63.5	0,8	0.10	175±16	0.915	2.15×10^{-2}	0.898	16.8±1.5	157.2	27.9±2.6

TABLE III $E_\pi = 200 \pm 5$ Mev

Angular distribution of π^+ mesons scattered by hydrogen

Angle ϑ in the laboratory system (degree)	Distance from the centre of the target to last scintillator (cm.)	Thickness of aluminium filter (cm.)	Approximate magnitude of background $\frac{N_4(\text{Dewar})}{N_4(\text{Dewar}+\text{H})}$	"Net" hydrogen effect (per 10^6 countings of monitor)	K factor characterising the beam	Ω effective solid angle in the laboratory system. (sterad.)	ε detection efficiency for scattered mesons	$\left(\frac{d\sigma}{d\Omega}\right)_{\text{lab.}}$ differential cross-sections in the laboratory system (10^{-27} cm^2 sterad^{-1})	Angle θ in the centre of mass system (degree)	$\frac{d\sigma}{d\Omega}$ differential cross-sections in the centre of mass system (10^{-27} cm^2 sterad^{-1})
20	73.5	6.8	0.6	249 ± 21	0.930	1.68×10^{-2}	0.734	36.9 ± 3.2	26.3	22.1 ± 1.9
35	63.5	6.8	0.3	242 ± 16	0.931	2.23×10^{-2}	0.733	27.0 ± 1.9	45.3	17.5 ± 1.2
50	63.5	3.0	0.2	199 ± 12	0.960	2.22×10^{-2}	0.850	18.7 ± 1.2	63.5	13.6 ± 0.9
80	63.5	3.0	0.2	77.6 ± 6.4	0.949	2.18×10^{-2}	0.870	7.38 ± 0.75	96.5	7.13 ± 0.73
95	63.5	3.0	0.1	93 ± 11	0.930	2.13×10^{-2}	0.883	9.0 ± 1.1	111.2	10.2 ± 1.2
110	63.5	3.0	0.1	117.1 ± 8.3	0.964	2.14×10^{-2}	0.893	10.8 ± 0.8	125.8	14.1 ± 1.1
150	63.5	3.0	0.2	141 ± 10	0.940	2.18×10^{-2}	0.881	13.3 ± 1.0	157.4	22.8 ± 1.7

TABLE IV $E_\pi = 240 \pm 6$ Mev

Angular distribution of π^+ mesons scattered by hydrogen

Angle ϑ in the laboratory system (degree)	Distance from the centre of the target to last scintillator (cm.)	Thickness of aluminium filter (cm.)	Approximate magnitude of background $\frac{N_4(\text{Dewar})}{N_4(\text{Dewar}+\text{H})}$	"Net" hydrogen effect (per 10^6 countings of monitor)	K factor characterising the beam	Ω effective solid angle in the laboratory system (sterad.)	ε detection efficiency for scattered mesons	$\left(\frac{d\sigma}{d\Omega}\right)_{\text{lab.}}$ differential cross-sections in the laboratory system (10^{-27} cm^2 sterad^{-1})	Angle θ in the centre of mass system (degree)	$\frac{d\sigma}{d\Omega}$ differential cross-sections in the centre of mass system. (10^{-27} cm^2 sterad^{-1})
20	73.5	9.0	0.6	267 ± 25	0.999	1.69×10^{-2}	0.701	38.4 ± 3.7	26.8	22.0 ± 2.1
35	73.5	6.8	0.2	166 ± 12	0.999	1.69×10^{-2}	0.749	24.6 ± 1.6	46.3	15.4 ± 1.0
35	63.5	6.8	0.3	174 ± 18	0.999	2.25×10^{-2}				
50	63.5	3.0	0.3	155 ± 10	1.074	2.25×10^{-2}	0.823	13.3 ± 1.0	64.7	9.47 ± 0.68
80	63.5	3.0	0.3	59.9 ± 4.0	1.074	2.20×10^{-2}	0.862	5.00 ± 0.36	97.8	4.92 ± 0.35
95	63.5	3.0	0.2	59.7 ± 4.2	1.066	2.16×10^{-2}	0.865	5.10 ± 0.38	112.4	5.86 ± 0.44
110	63.5	3.0	0.3	60.4 ± 4.2	1.067	2.15×10^{-2}	0.877	5.10 ± 0.38	126.0	6.80 ± 0.51
150	63.5	3.0	0.2	97.5 ± 5.1	1.038	2.19×10^{-2}	0.900	8.12 ± 0.47	158.1	14.50 ± 0.84

TABLE V $E_\pi = 270 \pm 6$ Mev

Angular distribution of π^+ mesons scattered by hydrogen

Angle ϑ in the laboratory system (degree)	Distance from the centre of the target to last scintillator (cm.)	Thickness of aluminium filter (cm.)	Approximate magnitude of background $\frac{N_4\text{ (Dewar)}}{N_4\text{(Dewar+H)}}$	"Net" hydrogen effect (per 10^6 countings of monitor)	K factor characterising the beam	Ω effective solid angle in the laboratory system (sterad.)	ε detection efficiency for scattered mesons	$\left(\frac{d\sigma}{d\Omega}\right)_{lab.}$ differential cross-sections in the laboratory system (10^{-27} cm^2 sterad^{-1})	Angle θ in the centre of mass system (degree)	$\frac{d\sigma}{d\Omega}$ differential cross-sections in the centre of mass system (10^{-27} cm^2 sterad^{-1})
20	73.5	9.8	0.6	210 ± 16	1.042	1.69×10^{-2}	0.689	29.4 ± 2.4	27.5	16.4 ± 1.3
50	63.5	3.8	0.3	104.6 ± 6.4	1.025	2.26×10^{-2}	0.827	9.24 ± 0.61	65.7	6.52 ± 0.43
80	63.5	3.0	0.4	29.3 ± 2.6	1.026	2.23×10^{-2}	0.848	2.57 ± 0.24	98.8	2.52 ± 0.23
95	63.5	3.0	0.4	21.9 ± 3.8	1.032	2.15×10^{-2}	0.859	1.94 ± 0.34	113.3	2.26 ± 0.40
110	63.5	3.0	0.3	37.1 ± 2.9	1.028	2.16×10^{-2}	0.871	3.25 ± 0.26	126.8	4.46 ± 0.36
149	63.5	3.0	0.4	45.2 ± 3.2	1.021	2.19×10^{-2}	0.880	3.90 ± 0.29	157.7	7.22 ± 0.54

TABLE VI $E_\pi = 307 \pm 6$ Mev

Angular distribution of π^+ mesons scattered by hydrogen

Angle ϑ in the laboratory system (degree)	Distance from the centre of the target to last scintillator (cm.)	Thickness of aluminium filter (cm.)	Approximate magnitude of background $\frac{N_4\text{(Dewar)}}{N_4\text{(Dewar+H)}}$	"Net" hydrogen effect (per 10^6 countings of monitor)	K factor characterising the beam	Ω effective solid angle in the laboratory system (sterad.)	ε detection efficiency for scattered mesons	$\left(\frac{d\sigma}{d\Omega}\right)_{lab.}$ differential cross-sections in the laboratory system (10^{-27} cm^2 sterad^{-1})	Angle θ in the centre of mass system (degree)	$\frac{d\sigma}{d\Omega}$ differential cross-sections in the centre of mass system (10^{-27} cm^2 sterad^{-1})
20	73.5	11.0	0.6	186 ± 15	1.024	1.69×10^{-2}	0.672	27.2 ± 2.3	27.9	14.5 ± 1.2
35	63.5	6.0	0.3	174 ± 17	0.984	2.25×10^{-2}	0.804	16.6 ± 1.7	47.9	9.86 ± 0.99
50	63.5	5.0	0.3	96.1 ± 5.1	1.021	2.26×10^{-2}	0.829	8.55 ± 0.48	67.1	5.91 ± 0.33
80	63.5	2.0	0.5	21.1 ± 2.2	1.021	2.25×10^{-2}	0.908	1.72 ± 0.19	100.0	1.55 ± 0.17
95	63.5	3.0	0.4	22.8 ± 4.5	0.992	2.18×10^{-2}	0.850	2.10 ± 0.41	114.5	2.49 ± 0.49
100	63.5	2.0	0.3	29.1 ± 2.6	1.021	2.19×10^{-2}	0.906	2.44 ± 0.23	127.8	3.42 ± 0.32
130	63.5	3.0	0.3	26.0 ± 4.4	0.996	2.18×10^{-2}	0.875	2.33 ± 0.40	144.0	3.92 ± 0.67
149	63.5	2.0	0.4	30.1 ± 3.2	1.020	2.19×10^{-2}	0.915	2.50 ± 0.27	158.2	4.77 ± 0.52

TABLE VII $E_\pi = 310 \pm 10$ Mev

Angular distribution of π^+ mesons scattered by hydrogen in photoemulsion

Angle interval in the c.m. system (degrees)	Number of scattering events registered	$\frac{d\sigma}{d\Omega}$ differential cross-section in the c.m. system (10^{-27} cm^2 sterad^{-1})
10— 30	75	16.0±1.8
30— 50	101	11.5±1.2
50— 70	84	7.0±0.8
70— 90	47	3.4±0.4
90—110	30	2.2±0.4
110—130	28	2.4±0.5
130—150	35	4.0±0.6
150—170	27	5.8±1.1

Concerning other additional errors of unknown origin, it can be stated that total cross sections σ_t (π^+, p), independently determined by attenuation of the meson beam, are close to the values obtained by integrating differential cross sections. It is evident that such errors may hardly be substantial. However, some additional errors are pointed out by the magnitude of experimental point deviations from the "best" least square curves, as will be seen later.

In Table VII are given data referring to the angular distribution of 310 Mev π^+ mesons scattered by hydrogen in the photoemulsion based on observation of 427 π^+–p interactions in the angle interval 10°-170° (in the c.m. system).

While considering the results obtained, at first the greatly symplifying assumption was made that only S and P waves take part in the scattering, i.e. the angular distribution can be written as

$$\frac{d\sigma}{d\Omega} = a_0 + a_1 P_1(\cos\theta) + a_2 P_2(\cos\theta)$$

Corresponding coefficients at various energies determined by the least square method are shown in Table VIII.

In order to make a convenient comparison of the present data with previously published results of angular distribution measurements which at other energies were usually presented as $\frac{d\sigma}{d\Omega} = a + b\cos\theta + c\cos^2\theta$, Table IX gives the corresponding coefficients.

The last column of Table VIII contains the values of

$$M = \sum_i \left\{\frac{f(\theta_i) - \sigma(\theta_i)}{\Delta\sigma(\theta_i)}\right\}^2,$$

where $\sigma(\theta_i)$ is the measured differential cross section at angle θ_i with an experimental error $\Delta\sigma(\theta_i)$; $f(\theta_i)$ — is the value at angle θ_i of the function $a_0 + a_1 P_1(\cos\theta) + a_2 P_2(\cos\theta)$ obtained by the least square method. In the 8th column are given the expected values M^1, which are equal to the difference between the number of experimental points n and the number of free parameters m [12].

TABLE VIII

π^+ meson scattering by hydrogen. Coefficients of angular distribution

Meson energy (Mev)	$\frac{d\sigma}{d\Omega} = a_0 + a_1P_1(\cos\theta) + a_2P_2(\cos\theta)$			$\lambda^{-2}\frac{d\sigma}{d\Omega} = A_0 + A_1P_1(\cos\theta) + A_2P_2(\cos\theta)$			Expected value $M^1 = n - m$	M
	a_0 (10^{-27} cm^2 sterad^{-1})	a_1 (10^{-27} cm^2 sterad^{-1})	a_2 (10^{-27} cm^2 sterad^{-1})	A_0	A_1	A_2		
176±4	15.86±0.38	-0.84±0.76	13.5 ±1.1	1.926±0.047	-0.102±0.093	1.63±0.13	6	1.7
200±5	14.15±0.29	1.04±0.55	12.47±0.82	1.996±0.041	0.147±0.078	1.76±0.11	4	5.7
240±6	10.12±0.29	4.58±0.57	9.95±0.63	1.770±0.050	0.80 ±0.10	1.74±0.11	4	4.4
270±6	6.47±0.25	4.73±0.50	7.07±0.50	1.300±0.050	0.95 ±0.10	1.42±0.10	3	5.0
307±6	5.45±0.19	5.12±0.38	6.18±0.40	1.275±0.045	1.199±0.089	1.45±0.09	5	11.3
310±10	5.5 ±0.2	4.9 ±0.4	6.2 ±0.6	1.31 ±0.05	1.17 ±0.10	1.48±0.14	5	1.2

TABLE IX

π^+ meson scattering by hydrogen. Coefficients of angular distribution

Meson energy Mev	$\frac{d\sigma}{d\Omega} = a + b\cos\theta + c\cos^2\theta$			$\lambda^{-2}\frac{d\sigma}{d\Omega} = A + B\cos\theta + C\cos^2\theta$		
	a (10^{-27} cm^2 sterad^{-1})	b (10^{-27} cm^2 sterad^{-1})	c (10^{-27} cm^2 sterad^{-1})	A	B	C
176	9.14±0.42	-0.84±0.76	20.2 ±1.6	1.11±0.05	-0.10±0.09	2.45±0.19
200	7.92±0.36	1.04±0.55	18.7 ±1.2	1.12±0.05	0.15±0.08	2.64±0.17
240	5.15±0.22	4.58±0.57	14.93±0.95	0.90±0.03	0.80±0.10	2.61±0.17
270	2.93±0.15	4.73±0.50	10.59±0.75	0.59±0.03	0.95±0.10	2.13±0.15
307	2.36±0.14	5.12±0.38	9.26±0.60	0.55±0.03	1.20±0.09	2.17±0.14
310	2.4 ±0.2	4.9 ±0.4	9.3 ±0.9	0.57±0.05	1.17±0.10	2.21±0.21

TABLE X

π^+ meson scattering by hydrogen (E_π = 307 Mev). Coefficients of angular distribution

$\frac{d\sigma}{d\Omega} = a_0 + a_1P_1(\cos\theta) + a_2P_2(\cos\theta) + a_3P_3(\cos\theta) + a_4P_4(\cos\theta)$					$\lambda^{-2}\frac{d\sigma}{d\Omega} = A_0 + A_1P_2(\cos\theta) + A_2P_2(\cos\theta) + A_3P_3(\cos\theta) + A_4P_4(\cos\theta)$						
a_0 (10^{-27} cm^2 sterad^{-1})	a_1 (10^{-27} cm^2 sterad^{-1})	a_2 (10^{-27} cm^2 sterad^{-1})	a_3 (10^{-27} cm^2 sterad^{-1})	a_4 (10^{-27} cm^2 sterad^{-1})	A_0	A_1	A_2	A_3	A_4	M^1	M
5.49±0.21	5.22±0.49	6.05±0.61	0.43±0.58	-1.34 ± 0.52	1.285±0.049	1.22±0.11	1.42±0.14	0.10±0.14	-0.31 ± 0.12	3	1.4

As is evident from the Table, for energies 176, 200, 240 and 310 Mev the M values are close to the expected one. For the energy 307 Mev M substantially exceeds M^1. This is illustrated in fig. 12, 13, 14, 15, 16 and 17, where distributions of the type

$$\frac{d\sigma}{d\Omega} = a_0 + a_1P_1(\cos\theta) + a_2P_2(\cos\theta)$$

are shown together with the experimental cross sections.

Consequently, for meson energies 307 Mev, there is some point in approximating the experimental data with a function possessing a greater number of free parameters, i.e. with a function of the form

$$\frac{d\sigma}{d\Omega} = a_0 + a_1P_1(\cos\theta) + a_2P_2(\cos\theta) + a_3P_3(\cos\theta) + a_4P_4(\cos\theta).$$

This may mean, that at an energy as high as 300 Mev it is difficult to describe meson-nucleon scattering by S and P waves only. The importance, if any, of the D wave contribution to the scattering will be discussed later. Table X gives the coefficients of the angular distribution obtained by a least square approximation of a function with five free parameters.

In fig. 16 the dotted curve shows the angular distribution

$$\frac{d\sigma}{d\Omega} = \{5{,}49 + 5{,}22P_1(\cos\theta) + 6{,}05P_2(\cos\theta) + 0{,}43P_3(\cos\theta) - 1{,}34P_4(\cos\theta)\} \cdot 10^{-27}\text{cm}^2 \cdot \text{ster}^{-1}.$$

B. Total cross-sections

Values of total cross-sections are given in the Table XI. Indicated errors are standard deviations and include un-

certainties in the corrections which take into account the considerable solid angle subtended by the last counter, counting losses in the registering system and μ^+ meson contamination. The contribution of the integral

$$\int_0^{\theta = 8^0} \left\{ \left(\frac{d\sigma_\pi}{d\Omega} \right)_{lab} + \left(\frac{d\sigma_p}{d\Omega} \right)_{lab} \right\} d\Omega$$ to the total cross-

section varies from 4×10^{-27} to 6×10^{-27} cm^2 with an uncertainty of about 10^{-27} cm^2 at all energies. In the

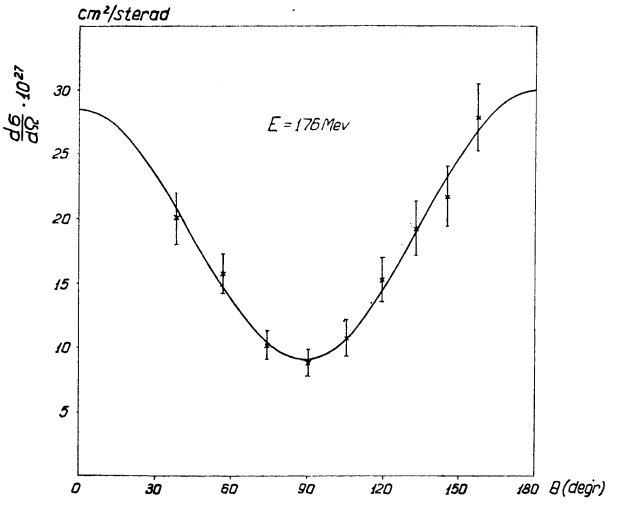

Fig. 12. Angular distribution of positive pions scattered by hydrogen (E_π = 176 Mev). The solid curve is the three parameters least square fit.

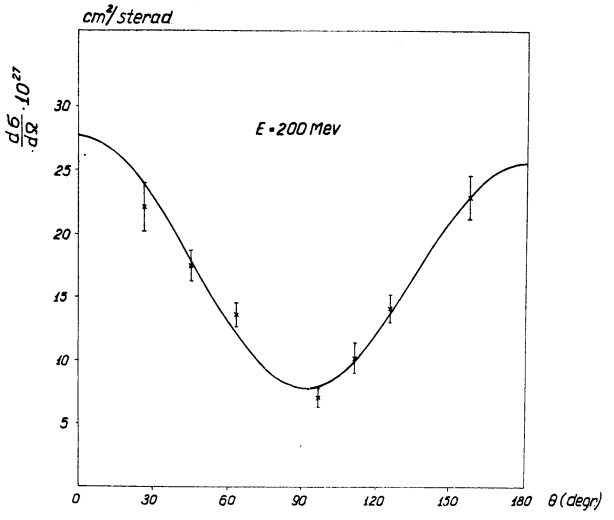

Fig. 13. Angular distribution of positive pions scattered by hydrogen (E_π = 200 Mev). The solid curve is the three parameters least square fit.

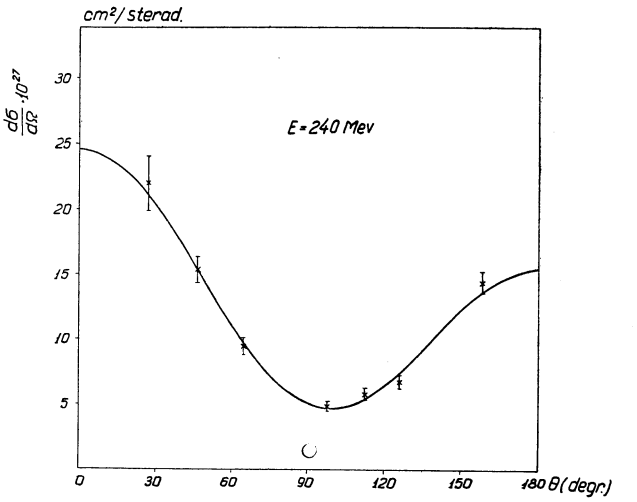

Fig. 14. Angular distribution of positive pions scattered by hydrogen (E_π = 240 Mev). The solid curve is the three parameters least square fit.

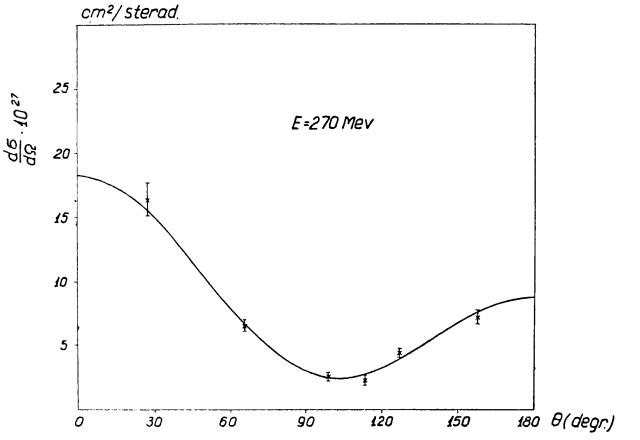

Fig. 15. Angular distribution of positive pions scattered by hydrogen (E_π = 270 Mev). The solid curve is the three parameters least square fit.

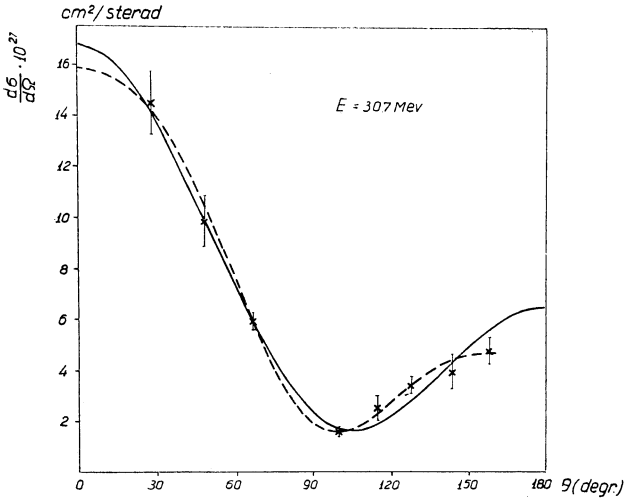

Fig. 16. Angular distribution of positive pions scattered by hydrogen (E_π = 307 Mev). The solid curve is the three parameter least square fit. The dotted curve is the five parameters least square fit.

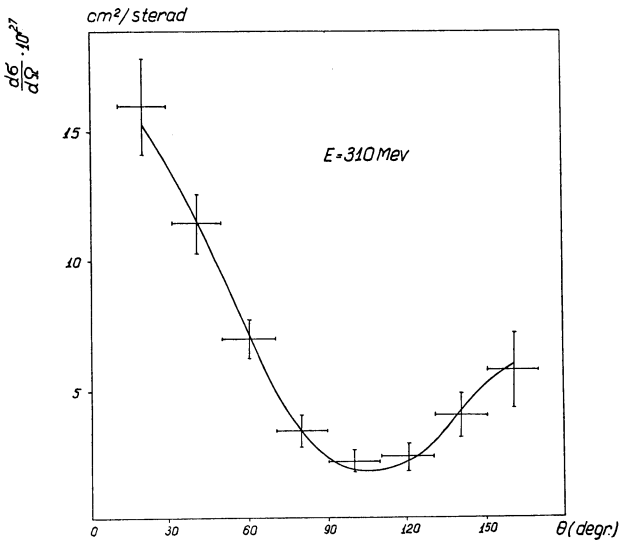

Fig. 17. Angular distribution of positive pions scattered by hydrogen (E_π = 310 Mev, photographic emulsion method). The solid curve is the three parameter least square fit.

same table in the third and fourth columns are shown values

$\sigma_t = \int \frac{d\sigma}{d\Omega} d\Omega$ obtained by the integration of functions

$$\frac{d\sigma}{d\Omega} = a_0 + a_1 P_1(\cos\theta) + a_2 P_2(\cos\theta) \text{ and}$$

$$\frac{d\sigma}{d\Omega} = a'_0 + a'_1 P_1(\cos\theta) + a'_2 P_2(\cos\theta) + a'_3 P_3(\cos\theta) + a'_4 P_4(\cos\theta)$$

with the coefficients which are shown in Tables VIII and X.

In fig. 18 together with the energy dependence of $\sigma_t(\pi^+, p)$ obtained by the beam attenuation method in our present and former [9] experiments the values of σ_t obtained by integrating differential cross-sections are given. It may be seen that the agreement of cross-section values obtained by two independent methods is good. There is some divergence only at energy 200 Mev. Comparison of these results with the data of other publications [13] is given in the following chapter.

TABLE XI

Total proton cross-sections for π^+ mesons

Meson energy (Mev)	σ_t (π^+,p) (10^{-27} cm²)	$\int \frac{d\sigma}{d\Omega} d\Omega = 4\pi a_0$ (10^{-27} cm²)	$\int \frac{d\sigma}{d\Omega} d\Omega = 4\pi a_0'$ (10^{-27} cm²)
176±4	193 ±6†	199.4±4.9	
200±5		177.9±3.7	
240±6	125.6±2.5	127.2±3.6	
270±6	85.2±3.0	81.3±3.1	
307±6	65.7±2.2	68.5±2.4	69.0±2.6

† Measurement made earlier [9] at energy 174 Mev.

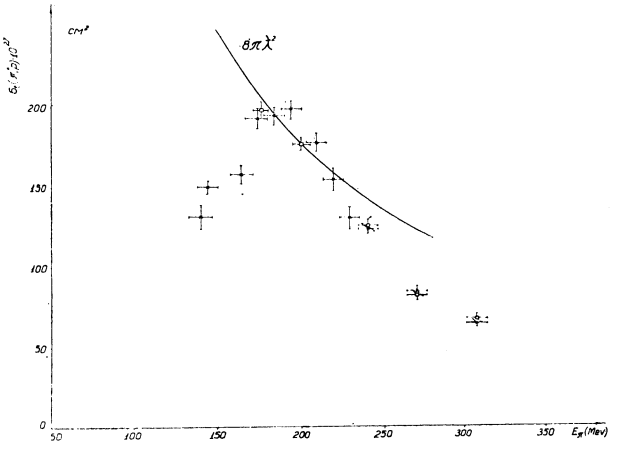

Fig. 18. Total positive pion cross-sections in hydrogen, obtained :
× By transmission.
□ By integration of angular distributions.

Discussion and interpretation of results

As is well known, Anderson et al. [14] have analyzed experimental data on π meson scattering at energies up to 200 Mev under the assumption that in the scattering only S and P waves take part and consequently that scattering processes are described by six phase shifts. In case of positive π mesons and in the absence of D waves the scattering is described by three phase shifts only α_3, α_{31} and α_{33}, determining the scattering respectively in the S, $P_{1/2}$ and $P_{3/2}$ states with isotopic spin $^3/_2$.

In this report data on positive meson scattering are analysed both on the assumption that the D state contribution in the scattering is negligible, i.e. that there is

appreciable interaction only in the S and P states (S-P analysis), and on the assumption that D state contribution is not negligible (S-P-D analysis). This last assumption may be justified at such high energies as 300 Mev. Besides, data shown in Table X do not contradict this assumption.

When S, P and D waves take part in π^+ meson scattering in addition to the formerly defined three phase shifts α_3, α_{31} and α_{33} there are 2 other phase shifts differing from zero; they correspond to D wave interaction in states with an angular momentum $^3/_2$ and $^5/_2$ and will be denoted by δ_{33} and δ_{35}.

I. *S–P Analysis*

A. Phase shifts

In case when π^+ meson interaction with hydrogen proceeds only through S and P states, analysis of the scattering is sufficiently simple and phase shifts in first approximation may be determined by a graphical method[15].

Angular distribution coefficients, as it is known, have the following form:

$$A=\sin^2\alpha_3+\sin^2(\alpha_{33}-\alpha_{31}) \quad (1)$$

$$B=2\sin\alpha_3[2\sin\alpha_{33}\cdot\cos(\alpha_{33}-\alpha_3)+\sin\alpha_{31}\cdot\cos(\alpha_{31}-\alpha_3)] \quad (2)$$

$$C=3\{\sin^2\alpha_{33}+2\sin\alpha_{31}\cdot\sin\alpha_{33}\cdot\cos(\alpha_{33}-\alpha_{31})\} \quad (3)$$

Results of the graphical analysis are given in Table XII. In the same table are shown "best" phase shifts [16] obtained with a fast electronic computer. As an independent measurement, total cross-section also was used in the analysis.

TABLE XII

Phase shifts in π^+ meson scattering by protons (in degrees)

Meson energy (Mev)	Graphical method			Electronic computer				Number of independent measurements
	α_3	α_{31}	α_{33}	α_3	α_{31}	α_{33}	M	
176	−11	−16	67	−10.6	−19.5	69.0	3.1	10
200	− 9	4′	96	− 9.1	10.0	102.0	7.0	7
240	−14	− 8	113	−18.1	− 2.6	114.7	4.2	8
270	−21	− 6	128	−20.2	− 6.7	129.3	5.8	7
307	−24	− 8	134	−23.2	− 8.4	133.2	12.0	9
310	−23	− 9	132	−22.7	− 7.1	131.3	1.1	8

In this table M denotes the quantity

$$\sum_i \left\{\frac{f_i(\alpha_3, \alpha_{31}, \alpha_{33}) - \sigma_i}{\Delta\sigma_i}\right\}^2.$$

Only the "resonance" solution was considered, i.e., the solution of the Fermi type in which α_{33} passes through 90° in the energy region 170-200 Mev. The basis for this was discussed in the work of Anderson et al.[17].

B. Behaviour of the S phase shift α_3 with the assumption that the scattering is determined by three phase shifts only

It is necessary to stress the fact that in the "resonance" region values of all three phase shifts are determined with low accuracy. As formulas (1), (2) and (3) show, α_{33} is very sensitive to small changes of coefficients A, B and C in the region where it is close to 90°. The difficulty in determining the S phase shift α_3 is due to the fact that the interference coefficient B, from which mainly this phase shift is being measured, is close to zero and in the "resonance" region is known with a very poor accuracy. At energies considerably exceeding "resonance", it is possible to determine both α_{33} and α_3 with a comparatively good accuracy. Therefore, special attention should be paid to the high values of the phase shift α_3 at energies of 240, 270, 307 and 310 Mev. The magnitude of this phase shift substantially exceeds values which could have been expected, if, up to these energies, the Orear [18] linear dependence of α_3 on meson momentum which describes quite well the experimental data at low energies, was valid. It is well known that Orear proposed the following phase shift equations:

$$\alpha_3 = -0{,}11\eta \quad (4)$$

$$(\eta^3/\omega)\cdot \mathrm{ctg}\alpha_{33}=8{,}05—3{,}8\omega \quad (5)$$

$$\alpha_{31}=0 \quad (6)$$

where η is the meson momentum in the c.m. system in units of μc, and ω is total energy minus the rest proton mass. Of course, not all the values of the "best" phase shifts satisfy the equations (4-6), but this may be due to uncertainties in the "best" phase-shift determinations of α_3 at energies close to "resonance". More specifically, Orear has shown that all known differential cross-sections up to 220 Mev do not contradict these equations.

In view of the theoretical interest of the behaviour of the S phase it is desirable to study the reasons of the observed deviation of α_3, at energies 240, 270, 307, and 310 Mev, from the linear dependence which is valid in the low energy region. The question may be put as to whether it is possible to explain the deviation only by the inaccuracy of the "best" values of the phase shift α_3. In order to answer this question, differential cross-section values (experimental values) shown in Tables II-VII were compared with the cross-section computed on the basis of

equations (4-6). Results of comparisons are shown in Table XIII.

TABLE XIII

Meson energy (Mev)	Number of experimental points	$M_{(4-6)}$
176	9	4.6
200	7	8.5
240	7	31
270	6	260
307	8	240
310	8	50†

† The difference in values $M_{(4-6)}$ at energies 307 Mev (electronics) and 310 Mev (photoplates) in no way indicates discrepancies in the measurement and is connected only with the different accuracy of these experiments.

In the last column are shown the values $M_{(4-6)} = \sum_i \left\{\frac{f(\alpha_3, \alpha_{33}, \theta_i) - \sigma(\theta_i)}{\Delta\sigma(\theta_i)}\right\}^2$ which characterize the degree of deviation of the curve $f(\alpha_3, \alpha_{33}, \theta_i)$, calculated with equations (4-6), from the experimentally measured values of differential cross-sections $\sigma(\theta_i)$.

The Table shows that experimental data at energies 176 Mev and 200 Mev do not contradict equations (4-6), a fact which confirms the analysis of other data in this energy region previously made by Orear. At higher energies it is absolutely impossible to satisfy experimental results with the phase shift values predicted by equations (4-6).

Supposing that up to energies of about 300 Mev scattering is sufficiently well described by S and P waves only, it may be definitely concluded from the foregoing that the linear dependence of α_3 on meson momentum, at energies exceeding 200-240 Mev, does not hold. On the other hand, since such a simple dependence is quite attractive, it is necessary to consider carefully whether experimental data can still be fitted with a linear dependence on momentum, by inserting a higher angular momentum (l=2), all the more so, since experimental data at energy 307 Mev indicate some difficulties in approximating the angular distribution with a function of type $a + b\cos\theta + c\cos^2\theta$ (see Tables VIII and XII).

II. *(S-P-D) Analysis*

When S, P and D waves take part in scattering the angular distribution can be written in the form

$$\lambda^{-2}\frac{d\sigma}{d\Omega} = A + B\cos\theta + C\cos^2\theta + D\cos^3\theta + E\cos_4\theta.$$

Phase shifts and angular distribution coefficients are related by the following equations

$$A = |S|^2 + |P_+ - P_-|^2 + |\tfrac{3}{2}D_+ + D_-|^2 - 2I(S/\tfrac{3}{2}D + D_+) \quad (7)$$

$$B = 2I(S/2P_+ + P_-) - 2I(\tfrac{3}{2}D_+ + D_-/2P_+ + P_-) + 6I(P_+ - P_-/D_+ - D_-) \quad (8)$$

$$C = |2P_+ + P_-|^2 - |P_+ - P_-|^2 + 9|D_+ - D_-|^2 - 6|\tfrac{3}{2}D_-|^2 + 6I(S/\tfrac{3}{2}D_+ + D_-) \quad (9)$$

$$D = 6I(2P_+ + P_-/\tfrac{3}{2}D_+ + D_-) - 6I(P_+ - P_-/D_+ - D_-) \quad (10)$$

$$E = 9|\tfrac{3}{2}D_+ + D_-|^2 - 9|D_+ - D_-|^2 \quad (11)$$

where the following notations are used:

$$S = e^{i\alpha_3}\cdot\sin\alpha_3;\ P_- = e^{i\alpha_{31}}\cdot\sin\alpha_{31};\ P_+ = e^{i\alpha_{33}}\cdot\sin\alpha_{33};$$

$$D_- = e^{i\delta_{33}}\cdot\delta_{33};\ D_+ = e^{i\delta_{35}}\cdot\sin\delta_{35};\ I(a/b) = \tfrac{1}{2}(ab^* + ab^*)$$

Total cross-sections are expressed in terms of phase shifts as follows:

$$\lambda^{-2}\frac{\sigma_t(\pi^+,p)}{4\pi} = \sin^2\alpha_3 + \sin^2\alpha_{31} + 2(\sin^2\alpha_{33} + \sin^2\delta_{33}) + 3\sin^2\delta_{35} \quad (12)$$

From the coefficients obtained at energy 307 Mev (Table X), the D wave phase shifts were roughly estimated in a preliminary way on the assumption that they are really needed. To simplify matters an approximate solution of equation systems (10) and (11) was sought for, in which it was supposed that $\alpha_{31} = 0$, and $\alpha_{33} = 134°$, i.e. equal to the phase shift α_{33} obtained by (S-P) analysis. This is a reasonable assumption, since the perturbation caused by D waves has little effect on α_{33}. It turned out that the obtained values of δ_{33} and δ_{35} can satisfy equations for all coefficients and, besides, it was found that the phase shift α_3 was considerably less than 24°, i.e. considerably less than the value obtained when S and P waves only were taken into account.††

†† It must be pointed out, that Orear long ago considered the effect of D waves [19] when interpreting experimental data on π-meson scattering by hydrogen in the region of energies up to 220 Mev. However, he took into account only the D wave with a total angular momentum $^5/_2$. As is evident from the equations (7-11), δ_{35} gives little "perturbation" on the phase shift α_3 if we assume δ_{35} of the order of a few degrees at energies 160-200 Mev.

The value $\delta_{35} = 0.013\ \eta^5$ proposed by Orear for fitting the experimental data in the region of energies from 100 up to 200 Mev, is excluded by the results of this report. Moreover, as has been shown by Orear himself [18], all experimental data in the region of energies up to 220 Mev are sufficiently well satisfied by equations (4-6), a fact which is confirmed also by our measurements (see Table XIII).

In view of this, experimental data presented in this report and also the data reported in other publications [2-5] have been analysed anew with the fast electronic computer BESM of the Academy of Sciences USSR. "Best" phase shifts α_3, α_{31}, α_{33}, δ_{33} and δ_{35} were obtained by considering only the solution in which α_3 is negative and α_{33} is within the limits of $\pm$ 10° from the values shown in Table XII.

In these calculations differential and total cross-sections were expressed by five phase shifts according to formulas (7-12). We tried to find the minimum of the following expression

$$M = \sum \left\{ \frac{f_i(\alpha_3,\alpha_{31},\alpha_{33},\delta_{33},\delta_{35}) - \sigma_i}{\Delta\sigma_i} \right\}^2,$$

where $f_i(\alpha_3,\alpha_{31},\alpha_{33},\delta_{33},\delta_{35})$ is the function expressing cross-section in terms of phase shifts and σ_i is the experimentally measured cross-section with the error $\Delta\sigma_i$. Phase-shift values, obtained by S-P analysis by means of the Ashkin diagrams, were used as initial data. As a first approximation the phase shifts beginning with α_3 changed in turn within the given limits by one degree. This cycle was repeated several times until the decrease of M stopped. Next, changes of half degree were made and so on. "Best" scattering phase shifts for energies 270 and 307 Mev obtained in this way are shown in Table XIV.

TABLE XIV

"Best" phase shifts (in degrees)

Meson energies (Mev)	α_3	α_{31}	α_{33}	δ_{33}	δ_{35}	M	Number of experimental points
270	-13.6	-4.3	128.8	4.3	-6.9	4.03	7
307	-13.0	-4.0	133.7	9.5	-10.0	3.78	9

As is shown in this table, experimental data at an energy of 307 Mev, which were poorly satisfied by three parameters (see Table XII), are well satisfied by five phase shifts. At this energy δ_{33} and δ_{35} are of the same order of magnitude in absolute values and have different sign. This circumstance may explain the fact, as it follows from relation (10), that the coefficient D, due to interference of P and D waves, is practically unobservable. As for the coefficient B it is due to the interference of S and P and also to the interference of P and D waves, wherefrom it follows that at all energies up to 300 Mev it is extremely difficult to determine separately the contributions of S and D waves.

A. D wave phase shifts δ_{33} and δ_{35}

It is impossible to make a definite statement about the magnitude of the D wave contribution at meson energies of about 300 Mev, only on the basis of the "best" solutions shown in Table XIV. Nevertheless, it is definitely important to consider the consequences such a solution leads to. This will be done further on, and, mainly, in considering the S phase behaviour.

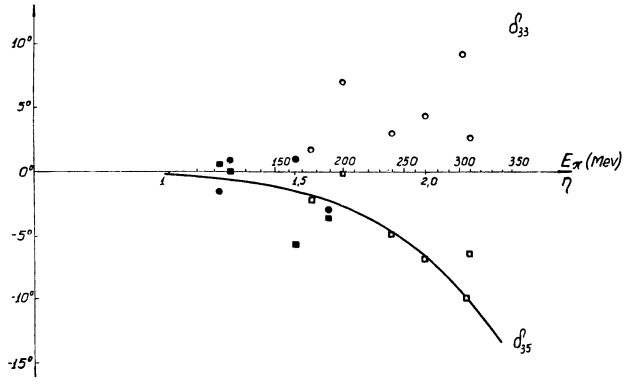

Fig. 19. D Wave phase shifts
δ_{33} { ○ Analysis of present experimental data. ● Analysis of data from other publications.
δ_{35} { □ Analysis of present experimental data. ■ Analysis of data from other publications.
Solid curve : $\delta_{35} = -0.21° \eta^5$.

As is known for small phase shifts, their dependence on meson momentum η in the centre of mass system may be written as const $\cdot \eta^{2l+1}$. Therefore, as a working hypothesis, the value of the D wave phase shifts were tentatively taken as $\delta_{33} = 0{,}20° \cdot \eta^5$ and $\delta_{35} = -0{,}21° \cdot \eta^5$, where coefficients are determined from the "best" values of phase shifts δ_{33} and δ_{35} at energy 307 Mev. Of course there is no justification for this, especially for the phase shifts δ_{33}, whose "best" values are not regular. In fig. 19 the dependence of δ_{35} indicated above is shown together with the "best" phase shifts δ_{35} and δ_{33}, obtained by means of the fast electronic computer. In the figure a tendency to increase the D wave phase shifts with increasing meson energy seems to be present, especially for δ_{35}. Taking into account the accuracy of initial data and the nature of the mathematical problem, it may be only stated that there is no contradiction between the dependence $\delta \sim \eta^5$ and the obtained data.

B. S-phase shift α_3

In fig. 20 are shown values of the α_3 phase shifts as a function of meson momentum η in the energy regions less than 100 Mev and greater than 240 Mev, i.e. in those regions of energy where this phase shift may be determined comparatively well. The straight line shows the dependence $\alpha_3 = -6{,}3° \cdot \eta$ which best of all satisfies experimental

data at low energies. Crosses denote values of α_3 at low energy. At high energies circles denote "best" values of α_3 obtained by supposing that only S and P waves take part in scattering.

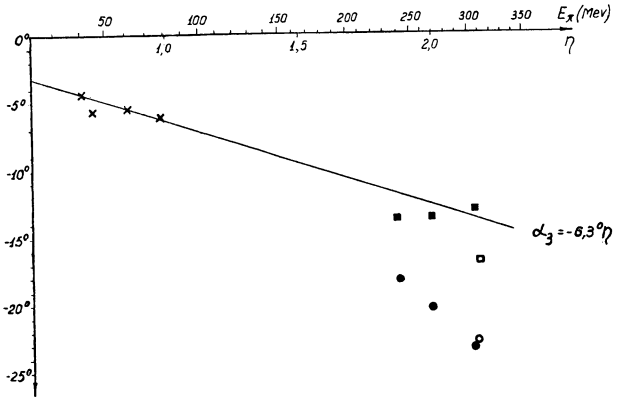

Fig. 20. Phase shift α_3 at low and high pion energies.
□ Photoplates (SPD-analysis).
■ Counters (SPD-analysis).
○ Photoplates (SP-analysis).
● Counters (SP-analysis).

From this figure it is evident that, as has been already indicated above, it is impossible to reconcile a linear dependence of α_3 with the phase shift values obtained in the region of high energies under S-P analysis. This would indicate that at energies greater than 200-240 Mev the meson wave length $\lambda\!\!\!^{-}$ (c.m. system) becomes comparable with the radius r_0 of the meson-nucleon interaction ($r^0 \sim \lambda\!\!\!^{-} \sim 0.8 \times 10^{-13}$ cm.).

In the same figure the squares show "best" values of α_3 for energies 240, 270, 307 and 310 Mev, obtained under SPD analysis. It is evident that these phase shift values are compatible with the Orear dependence suggested by the low energy experiments. This behaviour of the S phase shift suggests, but in no way proves, that already at energies of the order 300 Mev, when estimating the S phase shift, the D wave contribution might not be negligible.

Incidentally it might be mentioned that, if the dependence $\delta_{33} = 0{,}20^\circ\ \eta^5$ really were taking place, then already at energies 100-150 Mev there would be a marked influence of D waves on the coefficient B, from which the phase shift α_3 is mainly obtained. To illustrate this, in fig. 21 the solid curve shows the energy dependence of coefficient B, calculated by taking into account only S and P waves (α_3 was taken equal to $-\ 6.3^\circ\eta$), and the dotted curve shows the energy dependence of coefficient B, calculated taking into account the S, P and D waves ($\alpha_3 = -6{,}3^\circ \cdot \eta$ and $\delta_{33} = -\delta_{35} = 0{,}20^\circ \cdot \eta^5$). On the same figure values are given of coefficient B obtained at different energies by a least square method when angular distributions are approximated by a function of the type

$$\lambda\!\!\!^{-2}\ d\sigma/d\Omega = A + B\cos\theta + C\cos^2\theta.$$

It is evident that the linear dependence of α_3, in the form proposed by Orear, even at comparatively low energies better agrees with experimental data, when the contribution of D waves is taken into account.

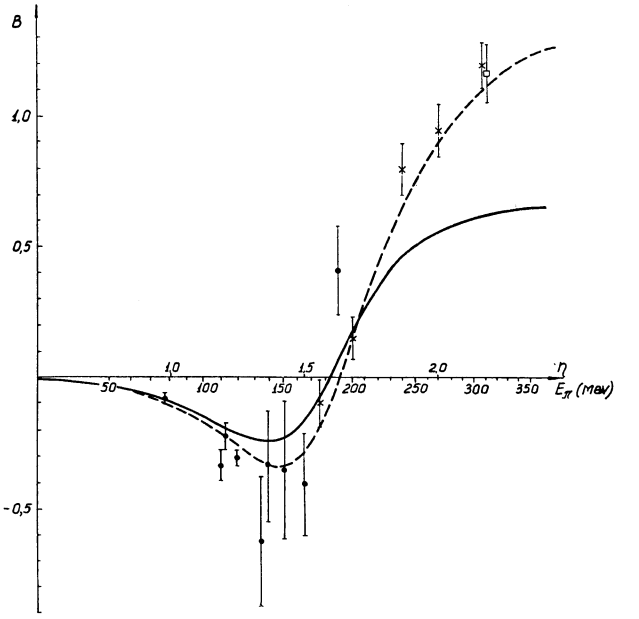

Fig. 21. Experimental points are values of the coefficient B obtained by least square approximation of type:

$$\lambda\!\!\!^{-2}\ \frac{d\sigma}{d\Omega} = A + B\cos\theta + C\cos^2\theta$$

See text for explanation of curves.

The linear dependence of α_3 which appears under the S-P-D analysis deserves special attention. As is known, phase shifts will be proportional to η^{2l+1} on condition that the radius r_0 of the meson nucleon interaction is shorter than the meson wave-length $\lambda\!\!\!^{-}$ in the centre of mass system. Consequently a linear or almost linear dependence of α_3 up to energy 307 Mev indicates that r_0 cannot be much larger than $\lambda\!\!\!^{-}_{(307\ \mathrm{Mev})} = 6.5 \times 10^{-14}$ cm.

Consequently, independently of whether only S and P waves are sufficient to describe the scattering process at about 300 Mev, from our measurements it follows that the radius r_0 of the meson-nucleon interaction is about 7×10^{-14} cm. Strictly speaking here r_0 is the radius of the meson-nucleon interaction in the S state with isotopic spin $^3/_2$. However, keeping in mind the experimental results on electron and proton scattering by protons [20], it is natural to link this value with the proton "dimensions".

C. Phase shift α_{31}

"Best" phase shifts α_{31}, formerly obtained by a number of authors, and also those obtained in the experiment described here at energies up to 220 Mev, are extremely chaotic, so that it is difficult to determine even the sign

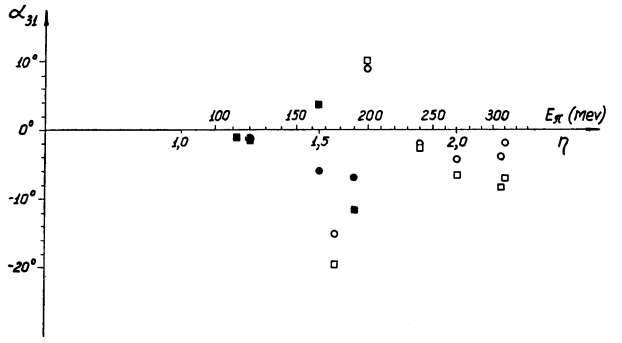

Fig. 22. Phase shift α_{31} at different energies.
□ Present work (SP analysis).
■ Present work (SPD analysis).
○ Previous publications (SP analysis).
● SPD analysis of data of previous publications.

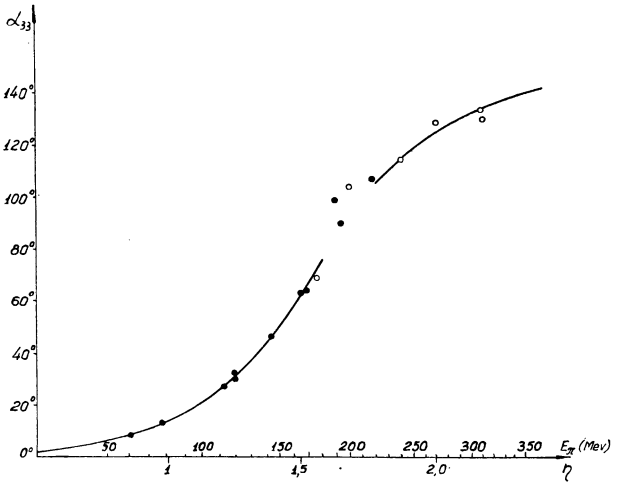

Fig. 23. Dependence of α_{33} on pion energy.
○ Present work
● Data from other publications
Solid curve : $\eta^3 \mathrm{ctg}\,\alpha_{33} = 4.3 + 0.6\,\eta^2 - 0.8\,\eta^4$

of this phase shift. However, in the region of higher energies the behaviour of phase shift is regular. From the data obtained in these experiments the definite conclusion may be drawn, that α_{31} is negative, and in all probability less than ten degrees up to 310 Mev. This is illustrated in the fig. 22, where the squares show "best" values of α_{31} obtained under S, P analysis and the circles denote "best" values of α_{31} obtained under S-P-D analysis. The figure shows that α_{31} is systematically decreasing when data are expressed by five phase shifts.

D. Phase shift α_{33}

Fig. 23 shows "best" phase shifts α_{33} obtained by a number of authors (see, for instance[5]). Circles denote "best" α_{33} values, obtained in these experiments under SPD analysis. It is necessary to point out that, when taking into account S and P waves only, phase shifts α_{33} differ slightly from those shown in figure. It is impossible to represent the data at energies higher than 240 Mev in the form of a straight line on a diagram of the Chew and Low type[21]. The theoretical significance of this fact is not clear to us, i.e. it is not clear if this is a consequence of the very nature of the theory which neglects proton recoils.

As was to be expected, at high energies the values of α_{33} shown in fig. 23 definitely exceed values which may be obtained from total cross section data (see fig. 18 and also the article of Lindenbaum and Yuan[13]), by assuming that the interaction is entirely due to state $P_{3/2}$.

Since the α_{33} values in the "resonance" region are determined with poor accuracy, we made an attempt to obtain the dependence of this phase shift, requiring that at low energies the dependence $\alpha_{33}=0.235\eta^3$ [18] should be maintained, and at high energies, that the present experimental data are satisfied. We choose the dependence in the form $\eta^3 \cdot \mathrm{ctg}\alpha_{33}=4.3+0.6\eta^2-0.8\eta^4$, which is shown in fig. 23 by the solid curve. Naturally the dependence thus obtained probably does not describe the behaviour of α_{33} in the "resonance" region. The behaviour of α_{33} in this energy region is discussed below.

The data of Lindenbaum and Yuan [13] indicate that the maximum of σ_t (π^+, p) is placed at an energy $\sim$ 175 Mev, whereas the data obtained by us (see fig. 18) show this maximum to be roughly at energy $\sim$ 185 Mev. Taking into account the errors in both measurements, it is impossible to conclude that there is a definite discrepancy in the experimental results. However, the statement of Lindenbaum and Yuan that α_{33} can pass through 90° at an energy as low as 175 Mev can hardly be true in our opinion. As a matter of fact, if we are to confine ourselves to S and P waves, then, as is known, the coefficient B is given by :

$$B=2\sin\alpha_3[2\sin\alpha_{33} \cdot \cos(\alpha_{33}-\alpha_3)+\sin\alpha_{31} \cdot \cos(\alpha_{31}-\alpha_3)]$$

Considering that in the region of energies close to "resonance" α_3 is roughly equal to — 10° and α_{31} is negative and small, it is possible to assert that α_{33} does not exceed 80° when B=0. Fig. 21 shows that B cannot be equal to zero at an energy less than 176 Mev, and so it follows that the "resonance" energy could hardly be substantially less than 190 Mev. This conclusion confirms the analysis of Bethe et al.[23].

Causality

On the basis of the paper of Goldberger, Miyazawa and Oehme [24] on the application of the causality principle to meson-nucleon scattering, Anderson et al. [17] and also Sternheimer [25] obtained the energy dependence

of the real part of the forward scattering amplitude from all the data on total meson-proton cross sections.

The real part of the forward scattering amplitude obtained in this way was compared by Anderson, Davidon and Kruse with its expression in term of phase shifts up to the energy 220 Mev. The new data obtained in the present report enable us to continue the comparison up to the energy 310 Mev. Use was made of the phase shift values obtained under both S-P and S-P-D analysis.

If D_+ denotes the real part of the forward scattering amplitude and λ and $\lambda_{c.m.}$ respectively the meson wavelength in the laboratory system and in the centre of mass system, then

$$\frac{2\lambda}{\lambda^2_{c.m.}} \cdot D_+ = \sin 2\alpha_3 + \sin 2\alpha_{31} + 2(\sin 2\alpha_{33} + \sin 2\delta_{33}) + 3 \sin 2\delta_{35}.$$

Fig. 24 shows the results of the analysis of the data obtained in the present experiments and also results of the analysis of some data on π^+–p scattering of other authors[2–5].

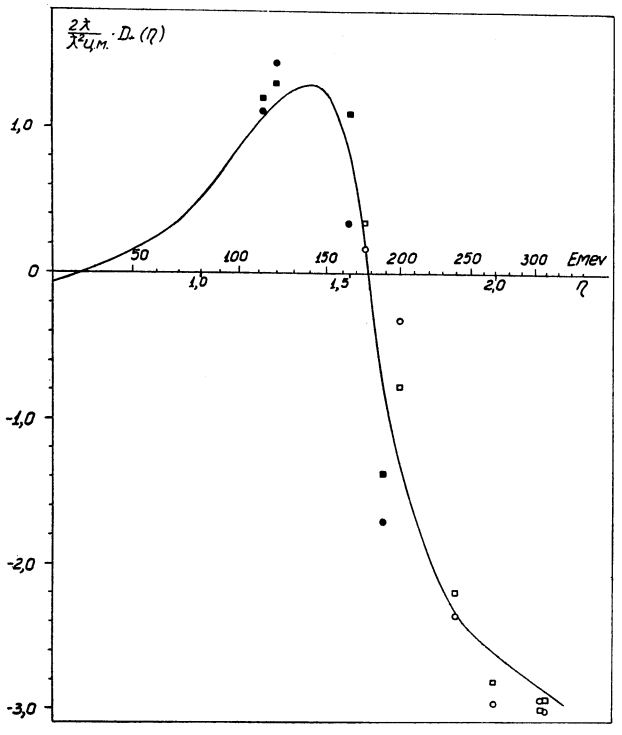

Fig. 24. Comparison of $\left(\frac{2\lambda}{\lambda^2_{c.m}}\right) D_+(\eta)$ calculated from causality conditions with :

$\sin 2\alpha_3 + \sin 2\alpha_{31} + 2(\sin 2\alpha_{33} + \sin 2\delta_{33}) + 3 \sin 2\delta_{35}$
- ○ Present work.
- ● Analysis of data of previous publications.

$\sin 2\alpha_3 + \sin 2\alpha_{31} + 2 \sin 2\alpha_{33}$
- □ Present work.
- ■ Previous publications.

From the figure it can be seen that the agreement between the real part of the forward scattering amplitude computed on the basis of causality conditions and its expression in terms of the phase shifts obtained from angular distribution in π^+–p scattering continues to remain very good up to the meson energy 310 Mev. It is impossible to give an answer to the question as to whether the results of the S-P analysis agree better with the computed curve than the results of SPD analysis. This could have been expected because the main features of the solid curve represented in the figure, even at energies $\sim$ 300 Mev, are determined by the phase shift α_{33}, which is equal in SP and SPD analyses.

Conclusion

A brief summary of the present work is given below.

1. Angular distributions of π^+ meson scattered by hydrogen, measured with scintillation counters at energies 176, 200, 240, 270, 307 Mev, and with photoplates at the energy 310 Mev, are shown in fig. 12-17.

2. The energy dependence of the total cross section $\sigma_t(\pi^+,p)$ is shown in fig. 18.

3. With a fast electronic computer a phase shift analysis of the data was made both on the assumption that the scattering process is described only by S and P waves (S-P analysis, Table XII) and on the assumption that S, P and D waves take part in the scattering (S-P-D analysis, Table XIV, figs. 19-22). Among the possible solutions, only that group of phase shifts was considered in which α_3 is negative and α_{33} passes through 90° in the region of energies 170-200 Mev.

4. The phase shifts α_{33} are shown in fig. 23. Practically they are identical in S-P and S-P-D analyses. Arguments are given to show that α_{33} passes through 90° at energy greater than 176 Mev.

5. The values of α_3 obtained by S-P analysis at energies 240, 270, 307 and 310 Mev are not compatible with Orear's equation $\alpha_3 = -0{,}11\eta$ which closely approximates the data at low energies.

6. There is no direct indication that an S-P-D analysis is necessary for the description of the data, except for the measurements made with scintillation counters at 307 Mev, which only with difficulty can be approximated by a function of the type $A+B\cos\theta + C\cos^2\theta$.

7. "Best" values of the phase shift α_{31}, which, as is well known, are chaotic up to energies $\sim$ 200 Mev, become regular at higher meson energies (fig. 22). It may be stated that α_{31} is negative and probably less than 10° up to 310 Mev. The phase shift α_{31} definitively decreases when data are expressed in terms of five phase shifts.

8. The "best" D wave phase shifts δ_{33} and δ_{35} are respectively positive and negative; they are shown in fig. 19, where it is possible to observe a tendency of these phase shifts to increase with meson energy.

9. Under S-P-D analysis the values of the S phase shift α_3 substantially decrease in comparison with its values obtained in S-P analysis (fig. 20). In fact when the data are analysed in terms of five phase shifts, α_3 depends on meson momentum linearly or almost linearly up to 310 Mev in agreement with the equation $\alpha_3 = -0.11\eta$.

10. Anyway, independently of whether 3 or 5 phase shifts are necessary to describe the scattering process at $\sim$ 300 Mev, from our experiments it follows that the radius r_0 of the meson nucleon interaction is $r_0 \sim 7 \times 10^{-14}$ cm. This conclusion is suggested by the deviation from linearity of α_3 in S-P analysis at energies from 200 to 240 Mev (conclusion 5), or, conversely by the very presence of the D wave, if S-P-D analysis is needed.

11. The real part of the forward scattering amplitude calculated from the causality conditions is in good agreement with its expression in terms of phase shifts up to 310 Mev.

The authors take pleasure in expressing their gratitude to E. I. Tamm and L. I. Lapidus for numerous discussions, to I. V. Popova and G. N. Tentucova for their great help in calculations, to B. S. Neganov and V. P. Zrelov for their aid in obtaining the meson beam and also to V. V. Krotov for his help in the measurements.

LIST OF REFERENCES

1. Bethe, H. A. and de Hoffmann, F. Mesons (v. 2 of Mesons and fields). New York 1955.
2. Ferretti, L. et al. Coulomb interference in the pion-pion scattering at 120 Mev. Nuov. Cim., *1*, p. 1238-50, 1955.
3. Orear, J. Measurement of Coulomb interference in 113 Mev π^+–p scattering. Phys. Rev., *96*, p. 1417-20, 1954.
4. Anderson, H. L. and Glicksman, M. Scattering of pions by hydrogen at 165 Mev. Phys. Rev., *100*, p. 268-78, 1955.
5. Anderson, H. L., Davidon, W. C., Glicksman, M. and Kruse, U. E. Scattering of positive pions by hydrogen at 189 Mev, Phys. Rev., *100*, p. 279-87, 1955.
6. Margulies, R. S. Positive pion scattering by hydrogen at 200, 300 and 400 Mev. Bull. Amer. phys. Soc., *30*, (7), p. 28, 1955.
7. Dmitrievski, V. P. et al. Report to All-Union conference of high-energy particles, May, 1956, Moscow.
8. Ignatenko, A. E., Mukhin, A. E., Ozerov, E. B. and Pontekorvo, B. M. (Total cross section for interaction of negative π mesons with hydrogen in the energy interval from 140 to 400 Mev.) Doklady Akad. Nauk SSSR, *103*, p. 45-7, 1955.
9. Ignatenko, A. E., Mukhin, A. I., Ozerov, E. B. and Pontekorvo, B. M. Zh. eksper. teor. Fiz. SSSR, *30*, p. 7- , 1956.
10. Ignatenko, A. E., Mukhin, A. I., Ozerov, E. B. and Pontekorvo, B. M. (Interaction of negative π mesons with beryllium, carbon and oxygen nuclei in the energy interval from 140 to 400 Mev.) Doklady Akad. Nauk SSSR, *103*, p. 395-7, 1955.
11. Ignatenko, A. E., Mukhin, A. I. Ozerov, E. B. and Pontekorvo, B. M. (Total cross section for interaction of negative π mesons with deuterium in the energy interval from 140 to 400 Mev.) Doklady Akad. Nauk SSSR, *103*, p. 209-12, 1955.
12. Rose, M. E. The analysis of angular correlation and angular distribution data. Phys. Rev., *91*, p. 610-5, 1953.
13. Lindenbaum, S. J. and Yuan, L. C. L. Total cross section of hydrogen for 150 to 750 Mev positive and negative pions. Phys. Rev., *100*, p. 306-23, 1955.
14. Anderson, H. L., Fermi, E., Martin, R. and Nagle, D. E. Angular distribution of pions scattered by hydrogen. Phys. Rev. *91*, p. 155-68, 1953.
15. Ashkin, J. and Vosko, S. H. Graphical methods for obtaining phase shifts from the experimental data on meson-nucleon scattering. Phys. Rev. *91*, p. 1248-51, 1953.
16. Mukhin, A. I., Pontekorvo, B. M., Popova, I. V. and Tentukova, G. N. Report to All-Union conference of high-energy particles May, 1956. Moscow.
17. Anderson, H. L., Davidon, W. C. and Kruse, U. E. Casuality in the pion-pion scattering. Phys. Rev., *100*, p. 339-43, 1955.
18. Orear, J. (*a*) Low energy behavior of the phase shifts in pion-proton scattering. Phys. Rev. *96*, p. 176-9, 1954.
(*b*) Energy dependence of the phase shifts in pion-proton scattering. Phys. Rev., *100*, p. 288-91, 1955.
19. Orear, J. A D-wave solution to pion-proton scattering data. Phys. Rev., *98*, p. 1155, 1955.
20. Smorodinski, Ia. A. (Dimensions of nucleons.) Uspekhi Fiz. Nauk, *56*, p. 425-8, 1955.
21. Rochester Conference on High energy nuclear physics. 5th, Proceedings, 1955. (See Chew, G. F. and Low, F. E.)
22. Brueckner, K. A. An application of the theory of the effective range to meson-nucleon scattering. Phys. Rev., *87*, p. 1026-30, 1952.
23. de Hoffmann, F., Metropolis, N., Alei, E. F. and Bethe, H. A. Pion-hydrogen phase shift analysis between 120 and 217 Mev. Phys. Rev., *95*, p. 1586-1605, 1954.
24. Goldberger, M. L., Miyazawa, H. and Oehme, R. Application of dispersion relations to pion-nucleon scattering. Phys. Rev., *99*, p. 986-8, 1955.
25. Sternheimer, R. M. Total cross sections for scattering and absorption of pions by nuclei. Phys. Rev., *101*, p. 384-7, 1956.

DISCUSSION

G. Puppi remarked that the plot showing the behaviour of α_3 has points at very low and at very high energy. Points are lacking in the intermediate region where there are deviations from linearity. The D wave which behaves like 0,2 η^5 is there very small and not sufficient to explain deviations from linearity.

A. I. Mukhin replied that these points are not indicated because α_3 is calculated by an electronic computer and depends mostly on the value of B. In this region B is very small and may be in error by perhaps as much as 200%.

G. von Dardel: "Is the highest energy used, 310 Mev, actually the highest where intensity is sufficient, or will measurements also be made at higher energies where D-waves would be even more important?"

A. I. Mukhin answered that at 310 Mev, the intensity of the meson beam obtained by the reaction $p+p \rightarrow \pi^+ + d$, is 40 mesons/cm² sec. To study angular distributions at higher energies one could use mesons produced by proton collisions on complex nuclei. But the analysis is made more difficult by inelastic processes such as:

$$\pi^+ + p \quad \begin{cases} \pi^+ + \pi^+ + n \\ \pi^+ + \pi^0 + p \end{cases}$$

which can occur at high energy.

J. Orear: "Did you find a larger ($\cos^4 \theta$) term than ($\cos^3 \theta$) term in your SPD analysis of both your data and that of the other laboratories?"

A. I. Mukhin said that the SPD analysis was made at 307 Mev only. It was found that $\delta_{33} \cong -\delta_{35}$. In this particular case $E > D$.

G. Bernardini asked what interaction constant was used in fitting theory to experimental results.

A. I. Mukhin answered that the fitting was made by use of the causality conditions as by Anderson at 240 Mev and Sternheimer at higher energy and does not require a coupling constant.